

ON THE APPROXIMATION OF THE REISSNER-MINDLIN PLATE BY THE p/hp VERSION OF THE FINITE ELEMENT METHOD

Christos Xenophontos^{*†}, Jason Kurtz[#], and Scott R. Fulton[#]

^{*} Department of Mathematical Sciences
 Loyola College

4501 N. Charles Street, Baltimore, MD 21210, U.S.A.

e-mail: cxenophontos@loyola.edu, web page: <http://www.evergreen.loyola.edu/~cxenophontos>

[#]Division of Mathematics and Computer Science
 Clarkson University
 Potsdam, NY 13699, U.S.A.

[†]Greek Association of Computational Mechanics

Keywords: Reissner-Mindlin plate, p/hp finite element method, shear locking, boundary layers.

Abstract. We study the approximation of the Reissner-Mindlin plate using the p/hp version of the finite element method (FEM). Our goal is to identify a method that: (i) is free of shear locking, (ii) approximates the boundary layer independently of the thickness of the plate and (iii) converges exponentially with respect to the number of degrees of freedom. We consider both standard and reduced constraint/mixed formulations, in the context of the p/hp version of the FEM, and we give guidelines for the construction of appropriate mesh-degree combinations that accomplish the above three goals, using straight as well as curved sided elements.

1 INTRODUCTION

The Reissner-Mindlin (R-M) plate model is a widely used system of partial differential equations, which describes the deformation of a thin plate subject to transverse loading. This two-dimensional model often replaces the full three-dimensional elasticity problem, when the thickness of the plate is small. To fix ideas, consider the bending of a homogeneous isotropic plate of thickness $t > 0$, occupying the region $\mathfrak{R} = \Omega \times (-t/2, t/2)$ where $\Omega \subset \mathbb{R}^2$ represents the midplane of the plate, under normal load density per unit area given by gt^3 . The equations of equilibrium for the rotation $\vec{\phi} = (\phi_1, \phi_2)$, and transverse displacement w , are

$$-\frac{D}{2}((1-\nu)\Delta\vec{\phi} + (1+\nu)\nabla\nabla\cdot\vec{\phi}) - \kappa\mu t^{-2}(\nabla w - \vec{\phi}) = 0 \quad (1)$$

$$\kappa\mu t^{-2}\nabla\cdot(\nabla w - \vec{\phi}) = g$$

where ν is the Poisson ratio, κ is the shear correction factor, E is the Young's modulus and

$$D = \frac{E}{12(1-\nu^2)}, \mu = \frac{E}{2(1+\nu)}.$$

Multiplying the top equation in (1) by t^2 , we see that the system is *singularly perturbed*. Hence, *boundary layers* will be present in the rotation (but not in the transverse displacement), as the thickness t tends to zero. Boundary layers, however, are not the only computational difficulty that one encounters when approximating the solution to the R-M plate model. As $t \rightarrow 0$, the solution $u := (\vec{\phi}, w)$ tends to the limiting solution

$u_0 := (\vec{\phi}_0, w_0)$, which satisfies *Kirchhoff's constraint*

$$\vec{\phi}_0 - \nabla w_0 = \vec{0}. \quad (2)$$

Practically, this means that the vertical fibers remain normal to the deformed midplane. The finite element solution must also satisfy a similar constraint and if the finite element space does have enough functions

satisfying (2), the approximate solution will be quite poor. This phenomenon is referred to as *shear locking* and conventional versions of the FEM can fail to overcome it. There are numerous papers aiming at designing “locking free” finite elements, (cf. ^{[2]–[12]} and the references therein), but only a handful address the use of high order p and hp versions of the FEM.

Our goal in this study is to address the question of how one can design a method that possesses three very important properties: (i) it is free of shear locking, (ii) it approximates the boundary layer independently of the thickness of the plate and (iii) it converges exponentially (or near-exponentially) with respect to the number of degrees of freedom. In Section 2 we address this question via a standard variational formulation, and discuss its advantages and disadvantages, in Section 3 we look at mixed/reduced constraint methods and in Section 4 we present our conclusions. Throughout the paper, we will use the usual Sobolev space notation $H^k(\Omega)$, denoting the space of functions on Ω with $0, 1, \dots, k$ generalized derivatives belonging to the space of square integrable functions, $L^2(\Omega)$. The norm and seminorm on $H^k(\Omega)$ will be denoted by $\|\cdot\|_{k,\Omega}$ and $|\cdot|_{k,\Omega}$, respectively. (The subscript indicating the domain will be dropped when no confusion occurs.) Finally, the letter C will denote a generic positive constant independent of the thickness t and any discretization parameters.

2 STANDARD FORMULATION

2.1 The finite element method

The standard variational formulation of (1) reads: Find $u_t := (\bar{\phi}_t, w_t) \in V = ([\Phi]^2 \times W) \subseteq [H^1(\Omega)]^2 \times H^1(\Omega)$ such that for all $v := (\bar{\theta}, \zeta) \in V$

$$A_t(u_t, v) := a_t(\bar{\phi}_t, \bar{\theta}) + \kappa \mu t^{-2} \langle \nabla w_t - \bar{\phi}_t, \nabla \zeta - \bar{\theta} \rangle = \langle g, \zeta \rangle \quad (3)$$

where $\langle \cdot, \cdot \rangle$ denotes the usual $L^2(\Omega)$ inner product and $a_t(\cdot, \cdot)$ is given by

$$a_t(\bar{\phi}, \bar{\theta}) := \frac{D}{2} \int_{\Omega} \left\{ (1-\nu) [\nabla \phi_1 \cdot \nabla \theta_1 + \nabla \phi_2 \cdot \nabla \theta_2] + (1+\nu) (\nabla \cdot \bar{\phi}) (\nabla \cdot \bar{\theta}) \right\} dx_1 dx_2. \quad (4)$$

The space V above can be made more specific once boundary conditions are specified. For example, in the case of a *clamped* plate (i.e. zero Dirichlet conditions on the boundary $\partial\Omega$), $\Phi = W = H_0^1(\Omega)$, where $H_0^1(\Omega) = \{u \in H^1 : u|_{\partial\Omega} = 0\}$, so that $V = [H_0^1(\Omega)]^2 \times H_0^1(\Omega)$.

The standard Galerkin finite element approximation of (3) proceeds by choosing a finite dimensional subspace $V^N = ([\Phi^N]^2 \times W^N) \subset V$, of dimension N , and seeking $u_t^N := (\bar{\phi}_t^N, w_t^N) \in V^N$ such that

$$A_t(u_t^N, v) = \langle g, \zeta \rangle \quad \forall v = (\bar{\theta}, \zeta) \in V^N. \quad (5)$$

We then have

$$\|u_t - u_t^N\|_{E,\Omega} = \inf_{v \in V^N} \|u_t - v\|_{E,\Omega}, \quad (6)$$

where $\|u\|_{E,\Omega} = (A_t(u, u))^{1/2}$ denotes the *energy* norm. It may be shown that there exist constants $\alpha_1, \alpha_2 > 0$ such that

$$\alpha_1 \|u\|_{1,\Omega} \leq \|u\|_{E,\Omega} \leq \alpha_2 t^{-1} \|u\|_{1,\Omega}$$

hence, for fixed $t > 0$, the two norms are equivalent.

We mentioned above that as $t \rightarrow 0$, the solution u_t tends to u_0 , which satisfies the constraint (2). The same constraint must be satisfied by u_t^N , in the limit, and if the space V^N does not have enough functions satisfying (2) the approximation will be quite poor. The finite dimensional subspaces V^N usually consist of piecewise polynomials on some subdivision (mesh) of the domain Ω . The dimension N can be increased to improve accuracy by refining the mesh (h version), increasing the polynomial degree (p version) or both (hp version). In this study we will only consider the p and hp versions, which were shown to be asymptotically *free* of locking, at least when quasiuniform meshes consisting of straight-sided elements are used (see ^[12]).

Due to the complicated nature of the interaction between the boundary layer and the locking effects, it is not completely clear how to precisely state a theorem that will describe the remedy and give bounds on the error. Instead, we will restrict ourselves to giving *guidelines* for the construction of the mesh-degree combination that

will yield satisfactory (numerical) results. To accomplish this task, we use the results of ^[1] that describe the exact nature of the boundary layer (in the case of plates with smooth boundary), hence allowing us to construct *a priori* mesh-degree combinations. In particular, it was shown in ^[1] that under sufficient smoothness on the loading function g and the boundary $\partial\Omega$, the solution $u_t = (\bar{\phi}_t, w_t)$ of (3) satisfies

$$u_t = u_0 + t u_k^S + t u_k^{BL} + u_k^R \quad (7)$$

where $u_0 = (\bar{\phi}_0, w_0)$ is the limiting solution satisfying (2), $u_k^S = (\bar{\phi}_k^S, w_k^S)$ is the smooth part of the solution, u_k^{BL} is the boundary layer part of the solution, and $u_k^R = (\bar{\phi}_k^R, w_k^R)$ is the smooth remainder. All derivatives of $\bar{\phi}_k^S, w_k^S, \bar{\phi}_k^R$ and w_k^R are uniformly bounded in t , and the boundary layer is given by

$$u_k^{BL} = (\chi \bar{\phi}_k^{BL}, 0) = \chi \sum_{i=1}^M t^i (\bar{\pi}_i(\rho/t, \theta) e^{-\sqrt{12\kappa}\rho/t}, 0) \quad (8)$$

where χ is a smooth cut-off function, (ρ, θ) are boundary fitted coordinates and $\bar{\pi}_i(\rho, \theta)$ are polynomials in ρ with (smooth in θ) coefficients. See ^[1] for details. The key observation is that (8) shows that the boundary layer effect is essentially one-dimensional, namely in the direction normal to the boundary. (This can be seen from the presence of the term $e^{-\sqrt{12\kappa}\rho/t}$.) Using the above results, it was shown in ^[13] that if $u_t^N = (\bar{\phi}_t^N, w_t^N)$ is the solution to (5), then

$$\|u_t - u_t^N\|_E \leq C \{ \mathfrak{S}_0(w_0, N) + \mathfrak{S}_1(u_k^S, N) + \mathfrak{S}_2(\chi u_k^{BL}, N) + \mathfrak{S}_3(\chi u_k^R, N) \} \quad (9)$$

where $C > 0$ is a constant independent of t and N , $\mathfrak{S}_0(w_0, N) = \inf_{v_0 \in V^N} \|u_0 - v_0\|_{E, \Omega} \leq C \inf_{z \in W^N} \|w_0 - z\|_{2, \Omega}$,

$\mathfrak{S}_1(u_k^S, N) = \inf_{v \in V^N} \|u_k^S - v\|_{E, \Omega}$, $\mathfrak{S}_2(\chi u_k^{BL}, N) = \inf_{\psi \in \Phi^N} \{ \|\chi u_k^{BL} - \psi\|_{E, \Omega} \}$ and $\mathfrak{S}_3(u_k^R, N) = \inf_{z \in V^N} \|u_k^R - z\|_{E, \Omega}$. Since \mathfrak{S}_1

represents the usual approximation rate of the space V^N and \mathfrak{S}_3 is usually bounded by \mathfrak{S}_1 for k large enough, the challenge lies in establishing $\mathfrak{S}_0 \leq \mathfrak{S}_1$ and $\mathfrak{S}_2 \leq \mathfrak{S}_1$. If the first inequality holds then our method is *locking-free*. If the second inequality holds then our method *approximates boundary layers uniformly* in t . In order to construct a method that incorporates all the observations made thus far, we use the mesh-design principles from ^[14], in the context of the p/hp version of the FEM, in order to construct a finite element scheme with *robust* approximation properties. These guidelines suggest that one element of width $O(pt)$, where p is the polynomial degree of the approximating shape functions, along the boundary of the domain is sufficient to fully capture the boundary layer effects. The use of the p/hp version of the FEM, allows us to (at least) expect the method to be asymptotically free of locking ^[12] (even though our meshes will not be quasiuniform and/or our elements will have curved sides). We refer to ^[15] for a detailed study of what happens in the presence of curved elements in the pre-asymptotic range of p . In the sub-section that follows we present the results of numerical computations using the above-mentioned guidelines, for two benchmark problems: a clamped rectangular plate and a soft simply supported circular plate.

2.2 Numerical computations on a rectangular plate

We consider the case of a clamped rectangular plate with $\Omega = [-1, 1] \times [-1, 1]$, loaded by $g = 1$, with Young's modulus $E = 1$ and Poisson ratio $\nu = 0.3$. The mesh is shown in Figure 1(a), and it includes *thin* elements (of width pt) along the boundary to capture the boundary layer effects; p is the degree of the approximating polynomial shape functions and t is the thickness of the plate. Strictly speaking, we should also include geometric refinement near each corner, to accurately approximate the corner singularities that will arise. In this problem, however, the singularities are not as severe as those that arise in, e.g. L -shaped domains ^[19], hence the boundary layer refinement will suffice. The polynomial degree was increased from $p = 1$ to $p = 7$, uniformly over all elements in the mesh. Note that the location, and not the number of elements changes with p , hence this is not the "true" hp version, but rather the p version on a properly designed (moving) mesh.

For all our computations, we will be interested in the (percentage) relative error in the energy norm

$$Error = 100 \times \frac{\|u_t^N - u_t\|_{E, \Omega}}{\|u_t\|_{E, \Omega}}, \quad (10)$$

as well as pointwise errors in the shear force

$$\vec{q} := [q_1(x, y), q_2(x, y)]^T = \kappa \mu t^{-2} (\nabla w - \vec{\phi}), \quad (11)$$

computed near the boundary of Ω . Figure 1(b) shows the (estimated) error, as given by (10), versus the number of degrees of freedom N , in a log-log scale for various values of the thickness. The error appears to be decreasing at an exponential rate, as p is increased, independently of t , hence the method is robust when the error in the energy norm is of interest. Note that, due to locking, p needs to reach the value of 5 in order for the error to decrease (see [12] for more details).

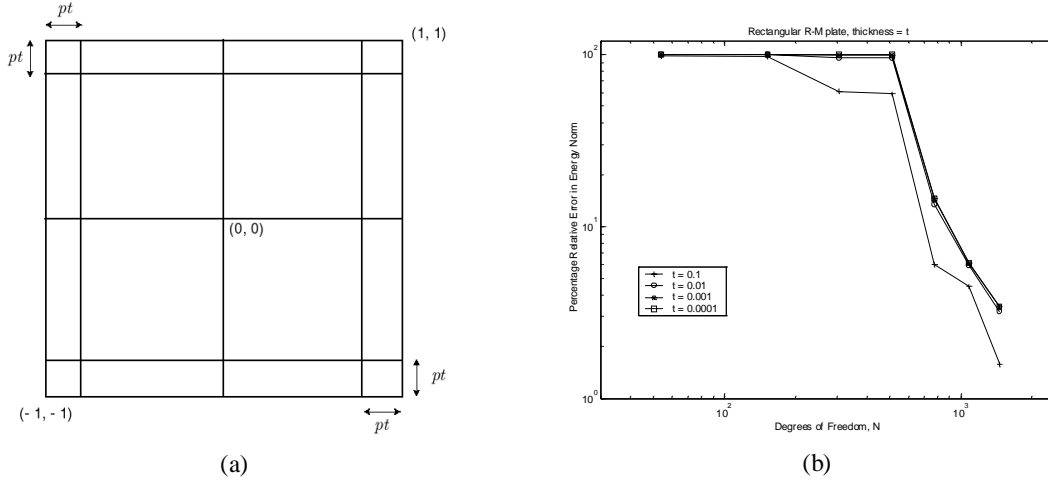


Figure 1. (a) Mesh for the rectangular plate. (b) Convergence of the standard method for the rectangular plate.

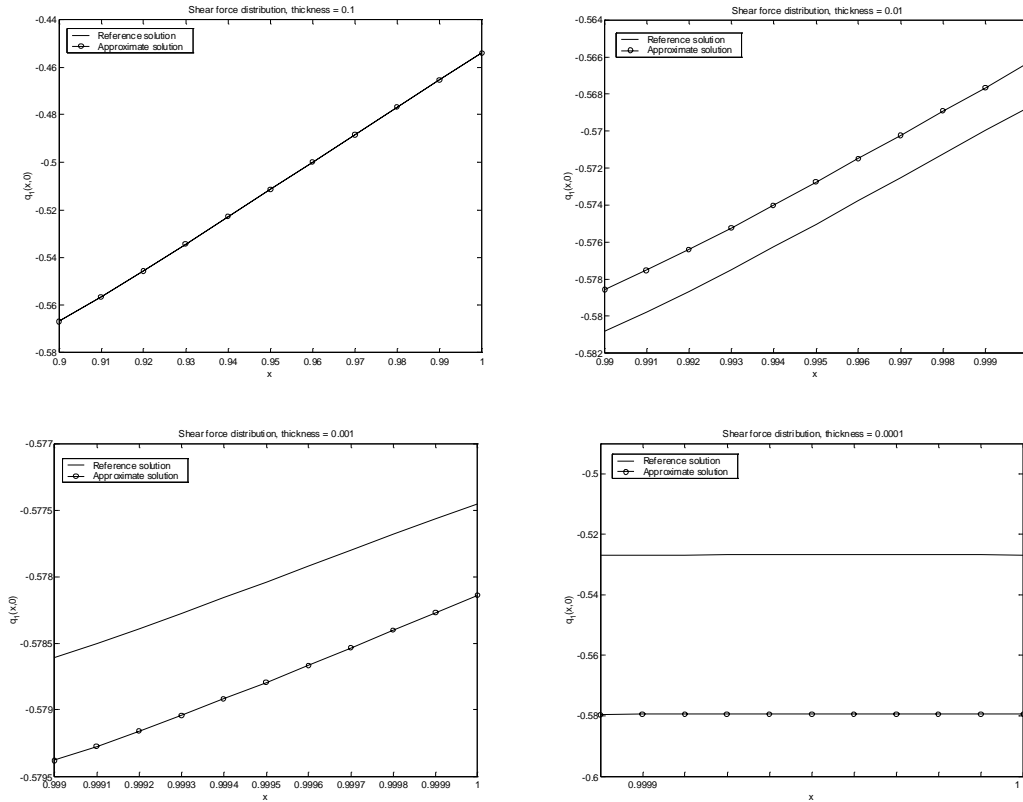


Figure 2. Shear force computation near the boundary for the rectangular plate (standard formulation).

Figure 2 shows the error in the pointwise shear force given by (11), near the boundary, for various values of t .

In particular, we plot $q_1(x, 0)$, $x \in (1 - t, 1)$, as predicted by our method using $p = 7$, along with a reference shear force obtained using a high(er) number of degrees of freedom. As these plots indicate, the method does not perform as well as it did in the energy norm, for small values of t , something that made researchers turn their attention to alternative approaches. As the results of our next experiment will show, the situation is worse when curved elements are used.

2.3 Numerical computations on a circular plate

We next consider the case of a soft-simply-supported circular plate with Ω being the unit disk, loaded by g given in polar coordinates by $g(\vartheta) = \cos(\vartheta)$, with Young's modulus $E = 1$ and Poisson ratio $\nu = 0.3$. Due to symmetry, the computations were performed on a quarter of the domain (see Figure 3(a)), with symmetry and anti-symmetry boundary conditions imposed on the lines $y = 0$ and $x = 0$, respectively, using the commercial finite element package StressCheck (E.S.R.D., St. Louis, MO). The degree p of the approximating polynomial was varied from 1 to 8, uniformly over all the elements in the mesh.

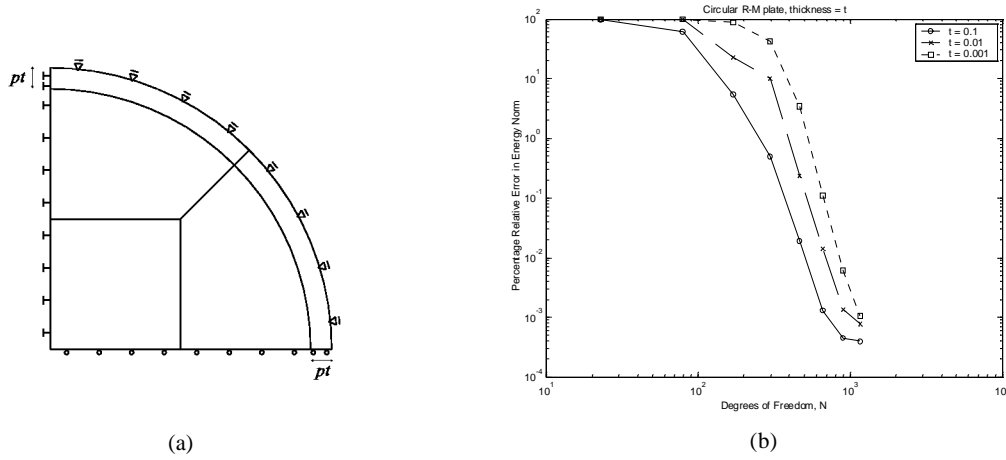


Figure 3. (a) Mesh and boundary conditions for the circular plate. (b) Convergence of the standard method for the circular plate

Figure 3(b) shows the error, as given by (10), versus the number of degrees of freedom N , in a log-log scale for various values of the thickness. The method appears to be converging at an exponential rate independently of t , as was the case with the previous example. We should note, however, that there is a “shift” in the error curves as t decreases, which is due to the enhanced locking because of the presence of curved elements (see ^[15], ^[17] for more details). When we look at the pointwise error in the shear force, as we did above, the situation is even worse. Figure 4 shows the pointwise shear force distribution near the boundary, $q_1(x, 0)$, $x \in (1 - t, 1)$, as predicted by our method (using $p = 8$), along with the exact shear (which is available from ^[18]). For relatively large values of t , there is very good agreement; as t decreases, however, the method does not yield satisfactory results, even though the error in the energy norm was small.

3 MODIFIED FORMULATION

3.1 Mixed Methods

One way to alleviate the shortcomings of the standard formulation when quantities of engineering interest (such as the shear force) are desired, is through the use of modified formulations, such as *mixed methods* or *reduced constraint methods*. In fact, the two approaches are, in some sense, equivalent. For a mixed method, the shear force (11) is introduced as an independent unknown and the following problem is solved: Find

$$u_t = (\vec{\phi}_t, w_t) \in V \text{ and } \vec{q}_t \in [L^2(\Omega)]^2 \text{ such that}$$

$$a(\vec{\phi}_t, \vec{\theta}) + (\vec{q}_t, \nabla \xi - \vec{\theta}) = (g, \xi) \quad \forall v = (\vec{\theta}, \xi) \in V$$

$$t^2 (\vec{q}_t, \vec{r}) - (\nabla w_t - \vec{\phi}_t, \vec{r}) = 0 \quad \forall \vec{r} \in [L^2(\Omega)]^2. \quad (11)$$

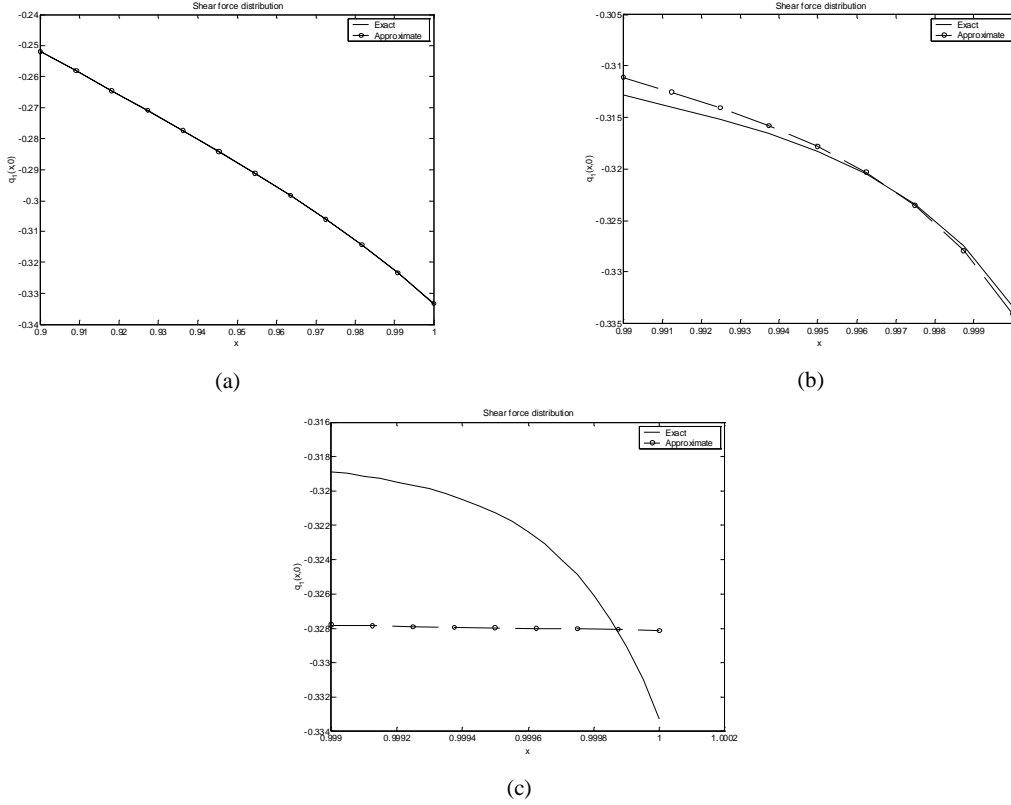


Figure 4. Shear force computation for the circular plate; (a) $t = 0.1$, (b) $t = 0.01$, (c) $t = 0.001$.

The discrete version arises by solving the above problem in finite dimensional subspaces $V^N \subset V$ and $Y^N \subset L^2(\Omega)$, as usual. The “trade-off” is that now in order for the best approximation result (6) to hold, we must establish the so-called Babuška-Brezzi (inf-sup) condition for each pair of subspaces V^N and Y^N chosen (see e.g. [6]). This was done for a large class of such pairs corresponding to the h version of the FEM, and for certain pairs of subspaces corresponding to the hp version of the FEM (in the case of quasiuniform meshes with straight sided elements [11]). Recently, some work has been done towards the use of these methods with non-uniform mesh strategies [15]–[17]), but to our knowledge, there is no (theoretical) result that combines the necessary mesh design with mixed methods and gives error bounds showing the robustness (and possible exponential rates of convergence) expected with this approach.

3.2 Reduced Constraint Methods

An equivalent approach to mixed methods is, instead of introducing additional unknowns, to weaken Kirchhoff’s constraint. This is done via a *reduction operator* $R_N : L^2(\Omega) \rightarrow S_N$, where S_N is a space of polynomials, that satisfies

$$R_N(\nabla \xi) = \nabla \xi \quad \forall \xi \in W^N.$$

We then solve the following problem (instead of (5)): Find $u_i^N := (\bar{\phi}_i^N, w_i^N) \in V^N$ such that

$$A_{i,N} := a_i(\bar{\phi}_i, \bar{\theta}) + \kappa \mu t^{-2} \langle R_N(\nabla w_i - \bar{\phi}_i), R_N(\nabla \zeta - \bar{\theta}) \rangle = \langle g, \zeta \rangle \quad \forall v = (\bar{\theta}, \zeta) \in V^N. \quad (12)$$

Note that by taking $R_N \equiv I$, we obtain the standard formulation (with $A_{i,N}(u, v) = A_i(u, v)$), and if $R_N \neq I$ we get a modified formulation. Various choices for R_N have been proposed in the literature (see [10] for an overview), varying from L^2 projections to more sophisticated choices involving mixed interpolation [4]. For the analysis, one has to bound a *consistency error*, in addition to the usual approximation error:

$$\|u_t - u_t^N\|_{E,\Omega} \leq C \left\{ \inf_{v \in V^N} \|u - v\|_{E,\Omega} + \sup_{z=(\psi,\zeta) \in V^N} \frac{|A_{t,N}(u, z) - (g, \zeta)|}{\|z\|_{E,\Omega}} \right\}. \quad (13).$$

For the calculation of the shear force, we use

$$\bar{q}^N := \kappa \mu t^{-2} R_N (\nabla w_t^N - \bar{\phi}_t^N) \quad (14)$$

which corresponds to a (trivial) post-processing scheme for \bar{q} . See ^[10] for more details, including an alternative post-processing scheme for the shear.

3.3 Numerical Results

The computations shown here correspond to the reduced constraint method, with R_N corresponding to the Raviart-Thomas spaces ^{[11], [12]}, and are for the rectangular plate considered in Section 2.2. We used the same mesh as before (see Figure 1(a)) and in Figure 5 we plot the error versus N in a log-log scale. The method seems to be converging at an exponential rate, as was the case with the standard formulation; in fact the error curves in Figures 3(b) and 5 are almost identical. The advantage of this approach is seen in Figure 6, which shows the shear force distribution, analogous to the results shown in Figure 2. We see that the predictions of this method do not deteriorate as t decreases and that the p/hp reduced constraint FEM with the appropriate mesh design allows us to accomplish the three goals stated in the Introduction.

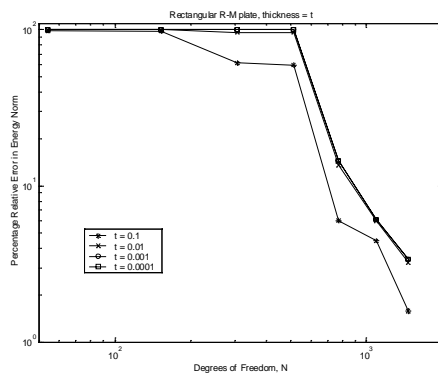


Figure 5. Convergence of error in the reduced constraint method for the rectangular plate.

4 CONCLUSIONS

We have studied the finite element approximation of the solution to the Reissner-Mindlin plate model and the computational difficulties associated with it, namely the presence of shear locking and boundary layer effects. Our numerical results indicate that the p and hp versions of the FEM perform very well, when combined with the proper mesh-design principles. When the error in the energy norm is of interest, both the standard and the modified variational formulations produced satisfactory results and the error decreased at an (observed) exponential rate. When the error in the shear force was considered, only the modified formulation gave good results. The question of “what happens when the modified formulation is used in conjunction with the p/hp version of the FEM on *curved* elements” is the focus of our current research efforts.

REFERENCES

- [1] Arnold, D. N. and Falk, R. S. (1996) “Asymptotic analysis of the boundary layer for the Reissner-Mindlin plate model”, *SIAM J. Math. Anal.*, Vol. 27, pp. 486 – 514.
- [2] Arnold, D. N. and Brezzi, F. (1989), “Innovative finite element methods for plates”, *Workshop on Innovative Finite Element Method, Rio De Janeiro, 27 November – 1 December*.
- [3] Arnold, D. N. and Falk, R. S. (1989) “A uniformly accurate finite element method for the Reissner-Mindlin plate”, *SIAM J. Num. Anal.*, Vol. 26, pp. 1276 – 1290.
- [4] Bathe, K. J., Brezzi, F. and Fortin, M. (1989) “Mixed interpolated elements for Reissner-Mindlin plates”, *Int. J. Numer. Meth. Eng.*, Vol. 28, pp. 1787 – 1801.
- [5] Brezzi, F. and Fortin, M. (1986) “Numerical approximation of Mindlin-Reissner plates”, *Math. Comp.*, Vol. 47, pp. 151 – 158.

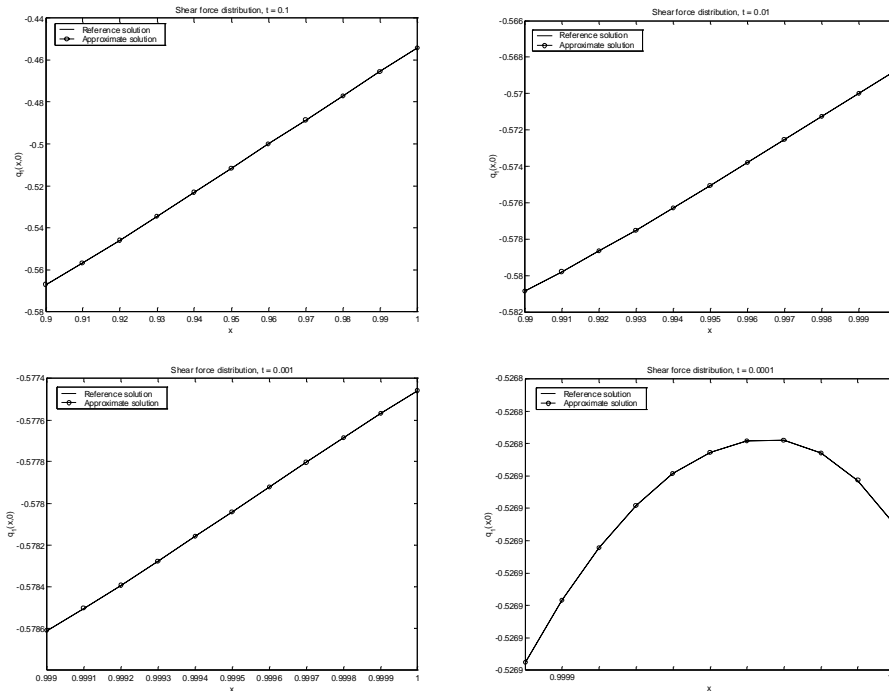


Figure 6. Shear force computation near the boundary for the rectangular plate .

- [6] Brezzi, F. and Fortin, M. (1991), *Mixed and Hybrid Finite Element Methods*, Springer-Verlag.
- [7] Brezzi, F., Fortin, M. and Stenberg, R. (1991), “Error analysis of mixed interpolated elements for Reissner-Mindlin plates”, *Math. Models and Methods in Applied Sciences*, Vol. 1, pp. 125 – 151.
- [8] Duran, R. and Liberman, L. (1992), “On mixed finite element methods for the Reissner-Mindlin plate model”, *Math. Comp.*, Vol. 58, pp. 561 –573.
- [9] Hughes, T. J. R. and Franca, L. P. (1988), “A mixed finite element formulation for Reissner-Mindlin plate theory: Uniform convergence of all higher-order spaces”, *Comp. Meth. Appl. Mech. Eng.*, Vol. 67, pp. 223 – 240.
- [10] Pitkäranta, J. and Suri, M. (1996), “Design principles and error analysis for reduced-shear plate bending finite elements”, *Numer. Math.*, Vol. 75, pp. 223 – 266.
- [11] Stenberg, R. and Suri, M. (1997), “An hp error analysis of MITC plate elements”, *SIAM J. Numer. Anal.*, Vol. 34, pp. 544 – 568.
- [12] Suri, M., Babuška, I. and Schwab, Ch. (1995), “Locking effects in the finite element approximation of plate models”, *Math. Comp.*, Vol. 64, pp. 461 – 482.
- [13] Schwab, C. and Suri, M. (1994), “Locking and boundary layer effects in the finite element approximation of the Reissner-Mindlin plate model”, *Proc. Symp. Appl. Math.*, Vol. 48, pp. 367 – 371.
- [14] Schwab, C., Suri, M. and Xenophontos, C. (1997), “The hp finite element method for problems in mechanics with boundary layers”, *Comp. Meth. Appl. Mech. Eng.*, Vol. 57, pp. 311 – 334.
- [15] Kurtz, J. and Xenophontos, C. (2002), “On the effects of using curved elements in the approximation of the Reissner-Mindlin plate model by the p version of the finite element method”, submitted to *Applied Numerical Mathematics*.
- [16] Ainsworth, M. and Pinchedez, K. (2001), “The hp -MITC finite element method for the Reissner-Mindlin plate problem”, submitted to *J. Comp. Appl. Math.*
- [17] Kurtz, J. (2002), “On the uniform approximation of the Reissner-Mindlin plate model by the p/hp version of the finite element method”, M.Sc. Thesis, Division of Mathematics and Computer Science, Clarkson University, Potsdam, NY.
- [18] Arnold, D. N. and Falk, R. S., “Edge effects in the Reissner-Mindlin plate model”, *Analytical and Computational Models for Shells*, A.S.M.E., New York, 1989.
- [19] Xenophontos, C. (1998), “Finite Element computations for the Reissner-Mindlin plate model”, *Comm. Numer. Meth. Eng.*, Vol 14, pp. 1119 – 1131.